Article:
Verch, A, Côté, AS, Darkins, R et al. (2014) Correlation between anisotropy and lattice distortions in single crystal calcite nanowires grown in confinement. Small, 10 (13). 2697 - 2702. ISSN: 1613-6810

https://doi.org/10.1002/smll.201303839

Correlation between Anisotropy and Lattice Distortions in Single Crystal Calcite Nanowires Grown in Confinement

Andreas Verch[1], Alexander S. Côté[2], Robert Darkins[2], Yi-Yeoun Kim[3], Renée van de Locht[1], Fiona C. Meldrum[3], Dorothy Duffy[2] and Roland Kröger[*1]

[1]Department of Physics, University of York, Heslington, York, YO10 5DD, United Kingdom

[2]Physics and Astronomy, University College London, London WC1E 6BT, United Kingdom

[3]School of Chemistry, University of Leeds, Leeds, LS2 9JT, United Kingdom

[*]Correspondence to: roland.kroger@york.ac.uk

Growing nanostructures in confinement allows for the control of their shape, size and structure, as required in many technological applications. We investigated the crystal structure and morphology of calcite nanowires, precipitated in the pores of track-etch membranes, by employing transmission electron microscopy and selected area electron diffraction (SAED). The data showed that the nanowires show no preferred growth orientation and that the crystallographic orientation rotated along the length of the nanowire, with lattice rotation angles of several degrees per micrometer. Finite element calculations indicated that the rotation is caused by the anisotropic crystallographic nature of the calcite mineral, the nanoscale diameter of the wires and the confined space provided by the membrane pore. This phenomenon should also be observed in other single crystal nanowires made from anisotropic materials, which could offer the potential of generating nanostructures with tailored optical, electronic and mechanical properties.

Keywords: Calcite Nanowires, Transmission Electron Microscopy, Finite Element Simulations, Crystallography

Many natural and technological processes involve the formation of crystals within constrained volumes rather than in bulk solution,[1,2] where confinement can affect key features such as morphology, size, single crystal/polycrystalline structure and polymorph selection.[3-6] Biomineralization is no exception to this, where the effects of soluble additives and the confined environments in which these materials form combine to generate the complex morphologies and hierarchical structures which characterise many biominerals. This results in crystalline materials with morphologies and properties quite distinct to their synthetic counterparts.[7,8]

In this paper, we present results which demonstrate that the formation of a crystal within a confined volume, as occurs during biomineralization,[2,9] can introduce intrinsic distortions in the material. Using transmission electron microscopy (TEM) in conjunction with selected area electron diffraction (SAED), a detailed analysis of the microstructure of calcite single crystal nanowires formed within the pores of track-etched membranes was performed. We show that 70 nm diameter nanowires exhibit significant crystal rotation along the length of the wire, while there is no detectable rotation found in 250 nm diameter calcite nanowires. It is emphasized that this cannot be attributed to the presence of dislocations, as in the case of the so-called "Eshelby Twist", which is attributed to a screw dislocation running up the core of the nanowire [10-12]. Here we demonstrate that an intrinsic surface stress induces lattice rotations in nanowires with anisotropic elastic properties and the magnitude of these rotations depend both on the crystallographic orientation and the diameter of the nanowires.

Results and Discussion

Calcite nanowires 5-10 μm in length were produced by precipitating $CaCO_3$ in the presence of poly(acrylic acid) (PAA) within the cylindrical pores of nominal diameters 50 nm and 200 nm polycarbonate track-etched membranes, as previously described.[13] In this method, the pores fill with amorphous calcium carbonate (ACC), which then transforms to single crystals of calcite, whose wire-like morphologies are defined by the membrane pores. Note that the pore sizes defined by the manufacturer are their diameters at the membrane surface.

After removal of the membrane material by dissolution in dichloromethane, (as described in Ref. 13), the nanowires were characterized in detail to determine their crystal structure and quality, the crystallographic direction corresponding to their long axes and the local lattice orientation. This information was obtained from TEM images and SAED patterns over a typical wire length of approximately 1-1.3 μm, where this was achieved by tilting one end of

a nanowire into a low index zone axis orientation. A sequence of diffraction patterns was then recorded in steps of 100 nm, from this position. The projected size of the SAED aperture used for these investigations was 125 nm. Examples of a nanowire and its diffraction pattern, which corresponds to a zone axis orientation of [2 4 1], are shown in Figures 1A and 1B respectively, with the white arrow in Figure 1B indicating the crystallographic orientation of the wire. The nearest reflection lying in the arrow direction represents a crystal plane perpendicular to the nanowire axis, and was used to determine the crystallographic direction of the long axis of the nanowire.

Scanning electron microscopy (SEM) overview images are shown in Figure S1. The diameters of the wires are in the range of 70 to 90 nm and, hence, are approximately 20-30 % thicker than the nominal diameters of the pores. The cylindrical shape of the wires was confirmed in all cases (see inset in Figure S1) indicating that the wire surfaces were not terminated by low energy facets, as expected for crystals grown from bulk solution, but fully molded to the shape of the membrane pores. The rough surfaces of the rods, which were previously described in some detail in reference is characteristic of crystallization from an amorphous precursor phase.[13]

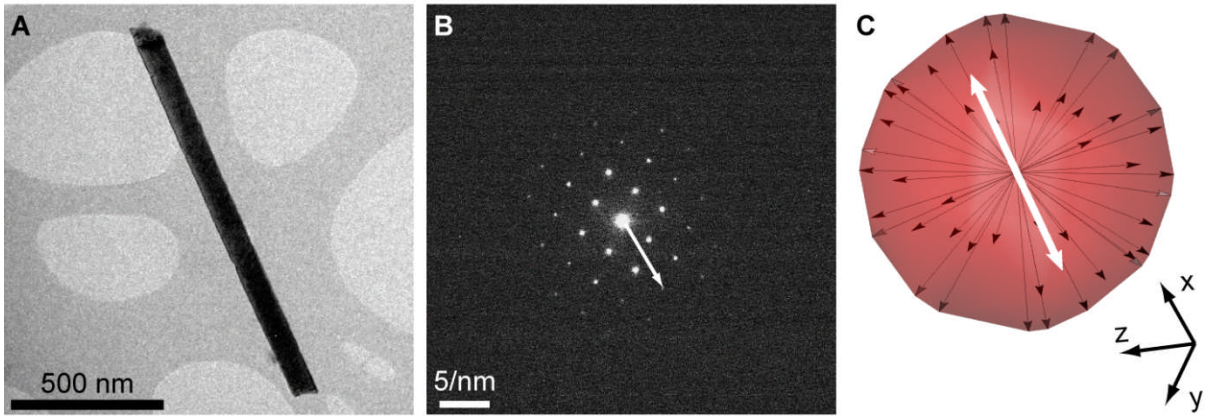

Figure 1: A TEM micrograph of a calcite nanowire. **B** Diffraction pattern of the wire shown in **A** in zone axis [2 4 1]. The white arrow indicates the growth direction of this wire, which is close to [20 4 -1]. **C** 3D-representation of the different growth direction of the wires studied in Cartesian coordinates, where the x-axis represents the a-axis of the unit cell and the y-axis the c-axis of the crystal. The bold white arrow indicates the growth directions of the wire shown in **A**.

Over 30 different nanowires were examined using this approach. In all cases, the diffraction patterns were identified as those of single crystal calcite along the complete investigated length, and no evidence for polycrystalline domains or other polymorphs was obtained. Analysis of this large population of nanowires also revealed a striking feature – that the crystallographic direction of the nanowire axis was entirely random. This isotropy of growth directions is visualized in Figure 1C, which shows a plot of the unit vectors of the determined wire orientations. The volume enclosing these vectors (shown in red in Figure 1C) is approximately spherical, which confirms the random orientation. These results demonstrate that the membrane surface does not direct the orientation of the crystal nucleus from which the product nanowire develops.

Nanowire formation from randomly oriented nuclei has been observed in other systems, mainly when using electrochemical deposition methods.[14] However, the resulting particles are usually not single crystals, but show polycrystalline characteristics.[15] In this context we can deduce from the observed single-crystallinity of the nanowires and their high aspect ratios that at the discussed length scales the crystallization process has to be significantly faster than the rate of nucleation, or that some degree of recrystallization can occur such that larger crystalline domains grow at the expense of smaller ones.

Most interesting, however, are the changes observed in the local lattice orientation along the length of the nanowires. The SAED pattern sequences show that there is a gradual change of intensity distribution as a function of position along the nanowire, indicating a change in the local crystal orientation. An example of this sequence for the nanowire shown in Figure 2A is presented in Figure 2C. This nanowire is oriented along a [-4 1 1] zone axis with a long axis close to [4 6 -3] and the red dots in Figure 2A show the positions of the patterns displayed in Figure 2C. The changes between patterns 1 and 7 are relatively small, while a sudden change

was observed between patterns 7 and 8, approximately 900 nm away from the wire end. This sudden change indicated a significant relative change in the lattice orientation at this position. The TEM image of a second nanowire, oriented along a [1 0 0] zone axis with its long axis is close to [2 4 1], as shown in Figure 2B. A dark-field TEM image using the (0 0 12) reflection is given in Figure 2D, demonstrating the presence of significant lattice rotation indicated by the non-uniform contrast. The SAED pattern sequence for this nanowire is shown in Figure S2.

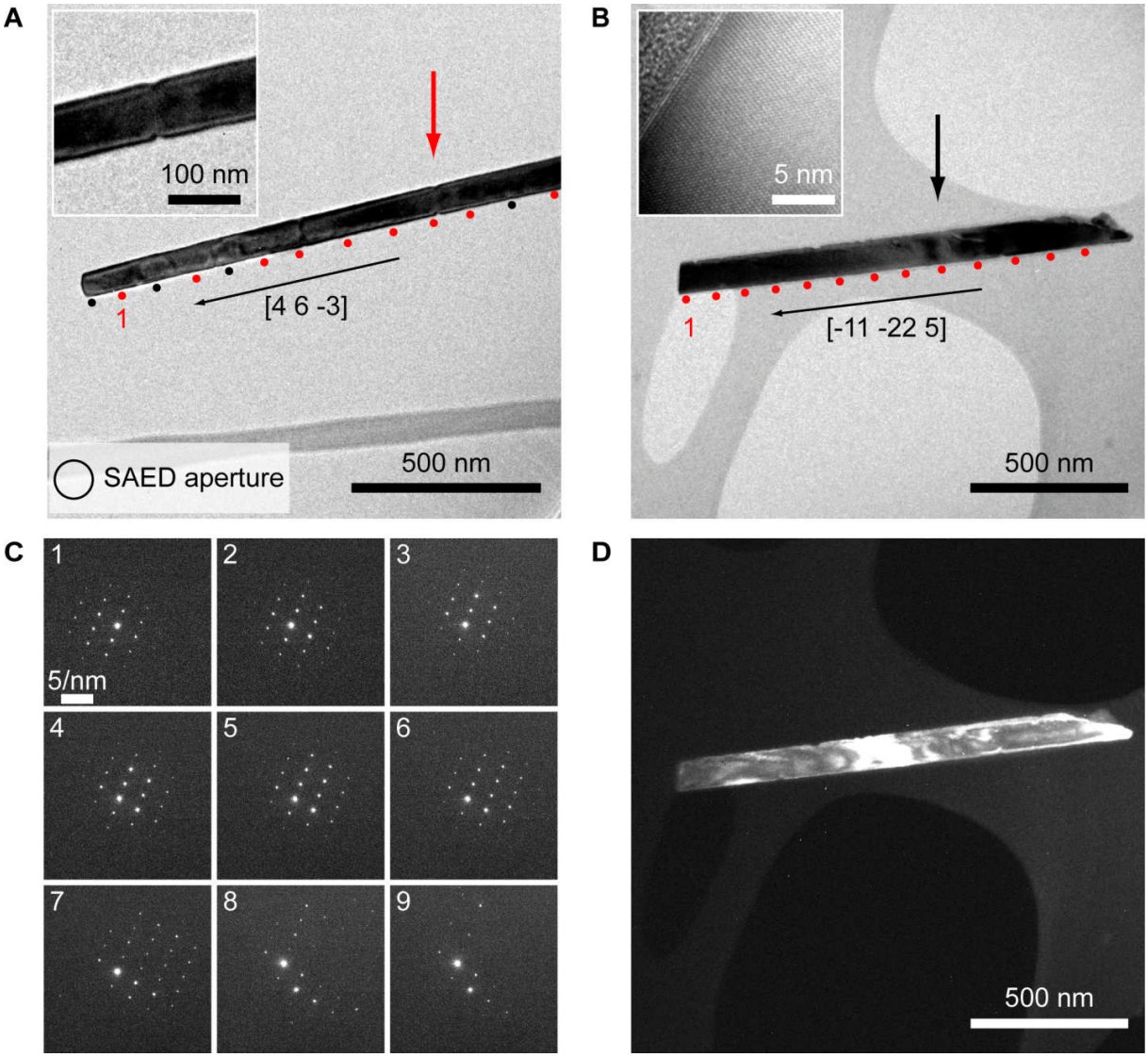

Figure 2: **A** TEM image of a wire with a growth direction close to [4 6 -3]. The red dots indicate the positions, where the diffraction patterns shown in **C** were recorded. Black dots indicate positions of additional diffraction patterns not shown in **C**. The size of the selected area diffraction (SAED) aperture is illustrated. The inset shows a pair of notches on the wire at the position indicated by the red arrow. **B** TEM image of wire with a growth direction close

to [-2 -4 1]. The inset shows a representative high-resolution TEM image taken near the surface area of the wire indicating a high crystal quality. **C** Series of diffraction patterns taken on the wire shown in **A** (zone axis: [-4 1 1]). **D** Dark field image of the wire shown in **B** using the (0 0 12) reflection illustrating the significant lattice rotation within the wire.

In order to quantify the lattice rotations displayed by these nanowires, three rotation axes were defined in the nanowire's frame of reference (inset in Figure 3A). These comprise a rotation angle α around the long axis of the nanowire (referred to as twist), a rotation angle β around the axis perpendicular to the wire and in the plane of observation (the out-of-plane bending), and an in-plane rotation γ around the zone axis. Based on kinematic diffraction pattern simulations,[16] the intensity distribution of the experimental patterns were compared with those obtained from the simulations at different rotation angles to obtain α, β and γ for each recorded diffraction pattern. These angles were then plotted as a function of the position along the nanowire. The errors in these measurements were approximately 0.1° for α and β, and 0.5° for γ. The larger error for γ is due to lens aberrations, which do not affect α and β.

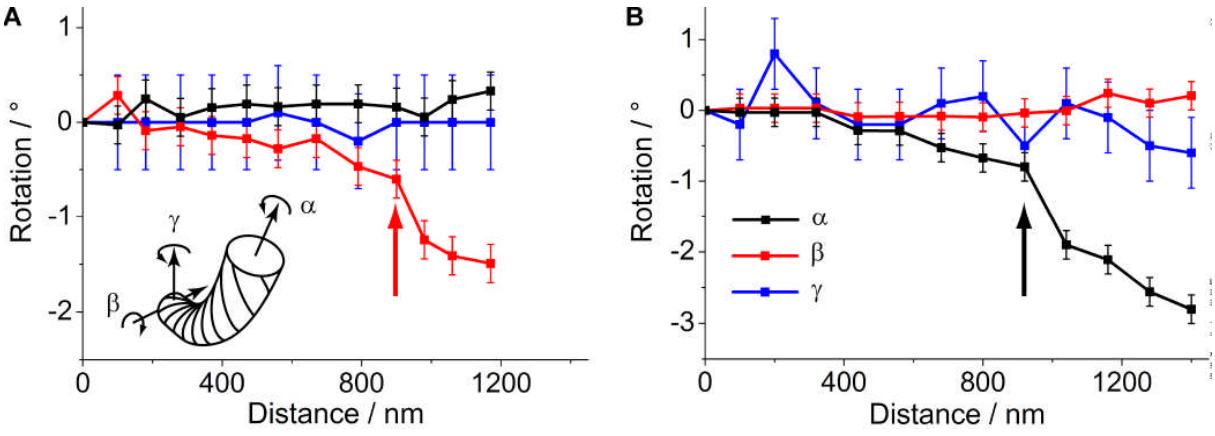

Figure 3: A and **B** show the rotations of α (black) , β (red) and γ (blue) as a function of the position for the two nanowires displayed in Figures 2A and 2B, respectively. The red and black arrows in **A** and **B** indicate positions of sudden changes of bend and twist, respectively.

The lattice rotations for the nanowires shown in Figures 2A and 2B are plotted in Figures 3A and 3B, respectively. A comparison of these figures demonstrates that the magnitudes of the three rotation angles along the length of a nanowire are specific to each nanowire. Thus, while the nanowire analyzed in Figures 2A and 3A shows little rotation of α and γ (where it is noted that the measurement of γ is associated with a larger error), the value of β reaches values of approx. 1.5° over 1200 nm. A closer inspection of the nanowire shown in Figure 2A reveales that the large increase of out-of-plane bending β at the wire position indicated by a red arrow, and shown at higher magnification in the inset, is associated with the presence of indents or notches. The origin of these notches remains unclear, but they may result from surface irregularities of the membrane pores. Such notches – often occurring in pairs – were observed in all nanowires with typical separations of 300 - 500 nm. It is noteworthy that not all observable notches were associated with sudden changes in lattice orientation and that in some nanowires sudden changes were observed that did not appear to be associated with notches. The nanowire shown in Figures 2B and 3B shows small β and γ rotations but the value of α reaches almost 3^{o} over 1400 nm, with a sudden change at 850 nm indicated by a black arrow in Figure 3B.

Additional results for wires grown in 50 nm track etch membranes are shown in Figure S3A-D and these clearly reveal the individual pattern of lattice distortions in each of them. For comparison, SAED studies single of crystal calcite nanowires precipitated in 200 nm diameter pores were also carried out. Importantly, none of these thicker nanowires showed detectable lattice rotations (see, for example, Figure S3E), clearly indicating that this effect is size-dependent.

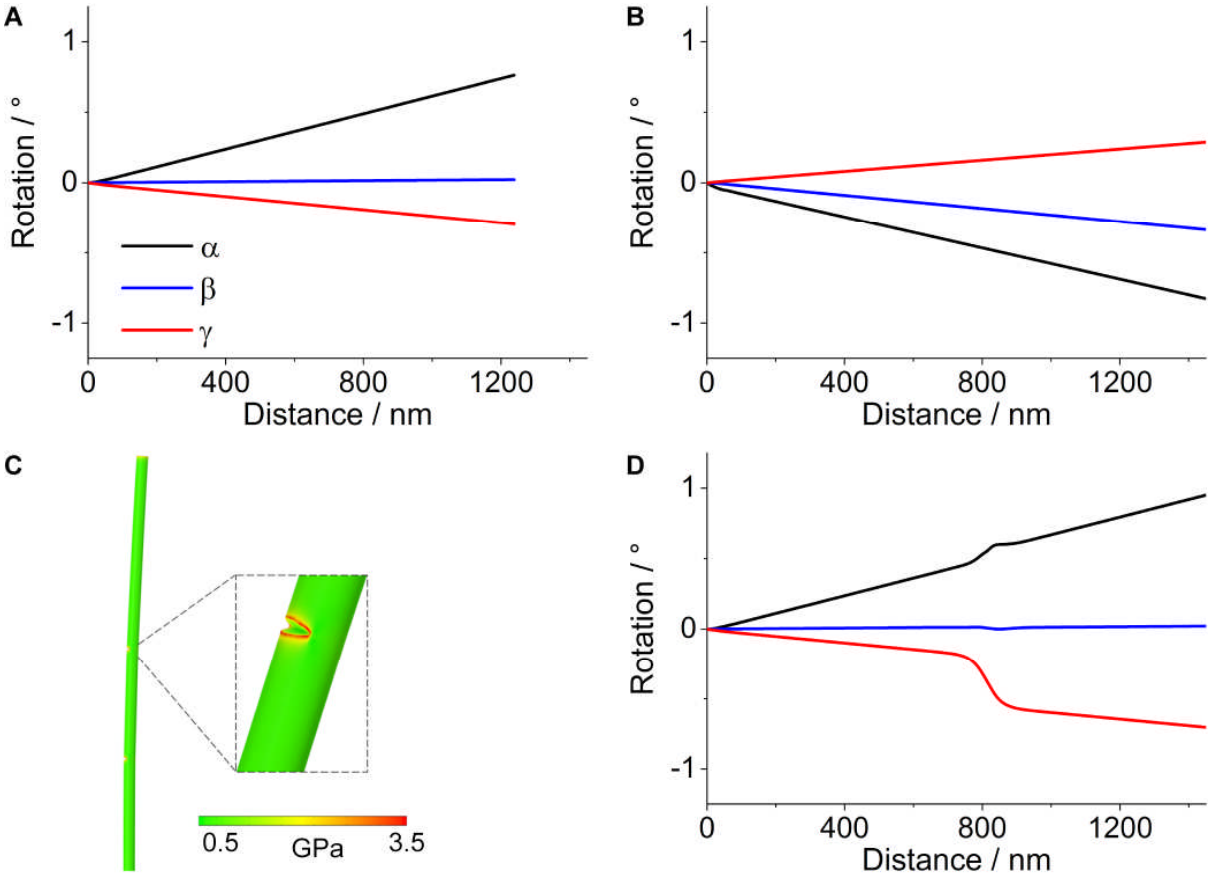

Figure 4: **A** and **B** show the results of the finite element calculations for nanowires with the same orientations as those shown in Figure 3 A and B, respectively. **C** shows the model used for the calculations in the presence of a notch on the surface and **D** shows the results of the calculations similar to 4A with a notch at 800 nm along the wire.

The observed crystallographic rotations must arise from residual stresses in the nanowires, originating either from the intrinsic structure of the wires after removal from the membrane or from defects. There was no evidence of extended defects (dislocations, twins or stacking faults). Therefore, we can rule out these features as the origin of the rotations. In general, crystal surfaces always induce residual stresses in crystals because the reduced coordination of the surface atoms induces structural relaxation of the atoms near the surface. Indeed, surface stress is known to be an important feature in nanostructures where the ratio of surface area to bulk volume is increased to such an extent that the surface stress results in bulk distortion. Typical examples include twisting of nanoribbons[17,18] and deformation of

nanowires and nanocantilevers[19-21]. The surfaces of the calcite nanowires are observed to be rough, therefore the induced stresses will be inhomogeneous and, typically, higher than those induced by flat surfaces.

To study the impact of uniform surface stresses on the lattice rotations we simulated 80 nm diameter nanowires with the elastic properties of calcite using finite element modeling (FEM). As the experimental wires all had different crystallographic orientations, and calcite is highly anisotropic, it was necessary to rotate the elasticity matrix for each individual orientation modeled. The surface was modeled by wrapping an 80 nm diameter nanowire with a 1nm thick membrane and compressing the membrane in the direction of the wire's axis. This surface stress induced a rotatory strain throughout all of the nanowires, the axis and magnitude of which varied with crystallographic orientation. Both bend and twist were exhibited in all of the nanowires except for the wire oriented in the [001] direction.

The results calculated using FEM for wires with crystallographic orientations corresponding to those presented in Figures 3A and 3B, for a homogeneous surface stress of 10 Nm^{-1}, are shown in Figures 4A and 4B. These calculations demonstrate that a 10 Nm^{-1} uniform surface stress gives lattice rotations with magnitudes roughly comparable to those observed experimentally over most of the nanowire length (i.e. neglecting the sudden changes). Surface stresses generally lie in the range 1-5 Nm^{-1},[22] therefore the value of 10 Nm^{-1} required to match the observed rotations is unrealistically high. The surfaces of the experimental nanowires are, however, observed to be non-uniform and this will result in a non-uniform surface stress. The effect of surface defects, such as the observed notches, was modeled (Figure 4C) and the resulting rotations are shown in Figure 4D. A surface stress with a higher value on one side of the nanowire than the other will induce the wire to bend. The large bend observed in the wire shown in Figure 3A was reproduced by FEM (Figure 5A) by imposing an inhomogeneous

surface stress that had a larger longitudinal component on one side of the wire compared to the opposite side (2 Nm^{-1} and 0.7 Nm^{-1}).

Calcite surface stresses are strongly anisotropic and this anisotropy will also have a significant effect on the lattice rotation as found e.g. for biogenic calcite, where anisotropy plays an important role in lattice distortions caused by organic inclusions.[23] We have calculated the surface stress tensors for a range of calcite surfaces, using an atomistic model, and found that a high degree of anisotropy, even for flat surfaces. As these calculations were carried out for smooth surfaces they are not an accurate representation of the rough surfaces of the experimental nanowires. Nevertheless they give a good estimate of the magnitude and anisotropy of surface stress that we use as input to the FE model. Our calculations show, for example, that the values of the principal stress components (i.e. the eigenvalues of the surface stress tensor) are -1.7 Nm^{-1} and +2.2 Nm^{-1} for the (018) calcite surface. In the case of the experimental nanowires the principal stresses are not necessarily directed parallel and perpendicular to the long axis of the wire, they will generally be at an arbitrary angle. FEM calculations demonstrate that an anisotropic surface stress, with principal components oriented at a finite angle to the long axis, always induces a twist component in the rotation of the wire. A calculation with an imposed surface stress with principal components of 2 Nm^{-1} and 1 Nm^{-1}, oriented at 30^{o} and 120^{o} to the long axis of the nanowire, gave rotations (shown in Figure 5B) very similar to the experimental values for the wire shown in Figure 3B. Thus we have shown that an inhomogeneous, anisotropic surface stress, combined with the elastic anisotropy of calcite, can explain the lattice rotations observed in the experimental nanowires. This is apparent from the good agreement between the measured and calculated rotations (Figures 3 and 5).

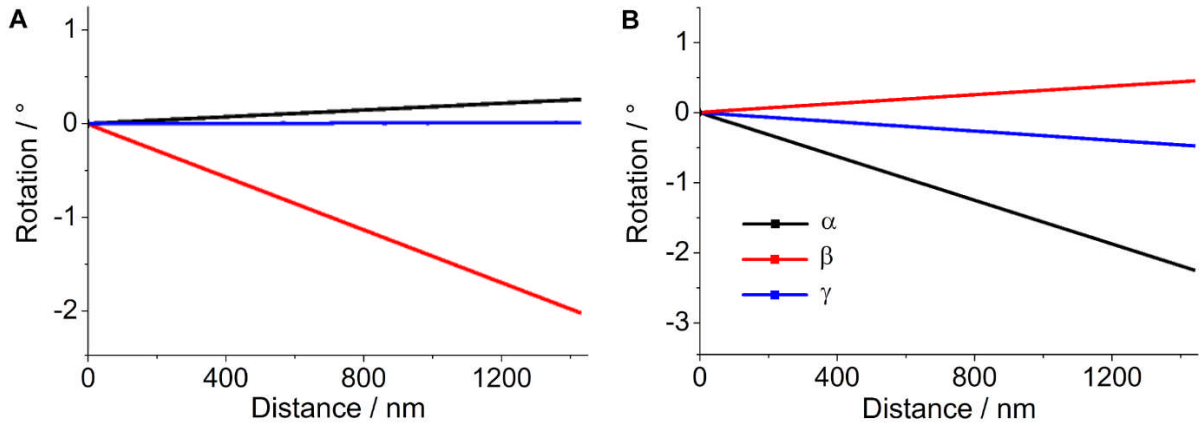

Figure 5: **A** Calculated rotations α (black) , β (red) and γ (blue) as a function of the position along the nanowire for a surface stress of 2 Nm^{-1} oriented along the wire on one side and 0.7 Nm^{-1} on the opposite side for a wire orientation corresponding to Figure 3A. **B** Calculated rotations for an anisotropic, surface stress with principal components of magnitudes 2 Nm^{-1} and 1 Nm^{-1}, oriented 30^{o} and 120^{o} to the axis of a nanowire orientated as in Figure 3B. In both cases the rotations agree well with the experimentally observed values.

Further insight into the nature of the stress fields responsible for the observed twisting and bending was obtained by employing linear elasticity theory to compute the stress field associated with a user-specified displacement field. This is a reverse approach to the finite element method, which computes displacement fields from stress fields. Using this methodology, we demonstrated that, irrespective of the crystallographic orientation, twisting is produced primarily by shear stress, and bending by tensile stress (Figure 6). The presence of both types of rotation can, therefore, be attributed to surface stress.

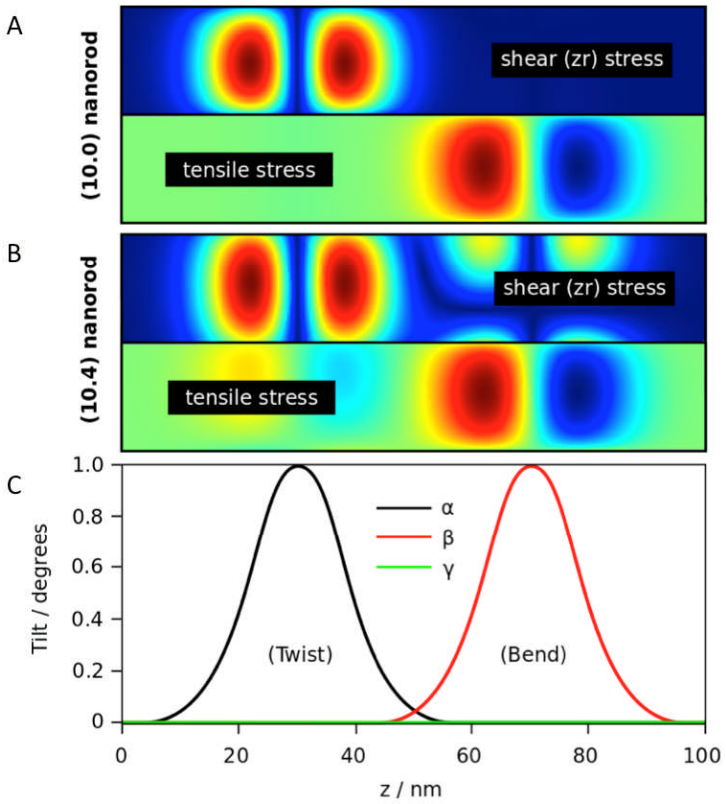

Figure 6: Polar plots of shear and tensile stress for A) [2 1 0] and B) [4 2 1] oriented wires corresponding to an arbitrary twist and an arbitrary bend (shown in C) each at different positions along the wire. (In the stress plots red and blue denote positive and negative values respectively, while green is zero). It is clear that twisting is strongly coupled with shear stress and bending with tensile stress.

We also profited from our modeling studies to rationalize the effects of the notches observed on the surfaces of several nanowires, which frequently corresponded to large changes in lattice distortion. The notches, modeled by carving small holes in the surface of the nanowire, introduced stress concentrations which accentuated the rotations resulting from the surface stress (Figure 4C,D). Such surface inhomogeneities could, together with locally varying surface stress, explain the observed inhomogeneous nature of the rotation along the length of the wire.

Conclusions

We investigated calcite nanowires grown in confinement using transmission electron microscopy and electron diffraction and found significant rotations of the crystallographic orientation along the length of the nanowire for wire diameters below 100 nm. Finite element modeling demonstrated that the observed rotations were consistent with those expected in anisotropic nanowires with surface stress values typical for ceramic materials with rough surfaces. In particular, we found that shear strain is necessary to create any significant twisting. The phenomenon we have observed in calcite is unique to anisotropic single crystal wires with nanoscale diameters, and it is notable that TEM analyses of calcite nanowires formed in bulk solution in the presence of poly(allylamine hydrochloride) (PAH) found no evidence for such lattice rotations.[24] The rough surfaces, due to crystallization in confinement, enhance the surface stress and inhomogeneities and, consequently, the magnitude of the induced rotation. Calcite is an important optical material and the rotation of the crystallographic orientation will affect the birefringence properties. It is expected that this phenomenon will also occur in a wide range of anisotropic semiconductor nanowires, such as ZnO, providing a mechanism for controlling or modifying the electronic bandgap for nanoelectronics. [25, 26]

Methods

A full description of the experimental methods is provided in the Supporting Information. Briefly, single crystal calcite wires were precipitated in polycarbonate track-etch membranes (Milipore) with cylindrical pores of either 50 or 200 nm diameter in the presence of poly(acrylic acid) (PAA) using established methods.[13] Wetted membranes were placed in a solution of $CaCl_2$ (10 mM) containing PAA (10 μg/ml), and $CaCO_3$ precipitation was induced

by exposure to solid ammonium carbonate in a closed desiccator. After incubation periods of 1-2 days, the intra-membrane crystals were isolated using at least 3 cycles of sonication in dichloromethane, centrifugation and solvent exchange, before being pipetted onto a TEM grid. The TEM experiments were conducted using a JEOL 2011 TEM-microscope operating at 200 kV. Finite element modeling of the calcite nanowires was used to calculate the elastic behavior of nanowires of similar diameters to the experimental wires.

Acknowledgements

This work was supported by the Engineering and Physical Sciences Research Council [grant number EP/I001514/1]. This Programme Grant funds the Materials Interface with Biology (MIB) consortium. RD acknowledges funding from EPSRC under the Molecular Modelling and Materials Science Industrial Doctorate Centre and the US Department of Energy (DOE), Office of Basic Energy Sciences, Division of Materials Sciences and Engineering, under Award KC020105-FWP12152.

References

1. Addadi, L., Joester, D., Nudelman, F., Weiner, S. Mollusk Shell Formation: A Source of New Concepts for Understanding Biomineralization Processes. *Chem. Eur. J.* **2006,** *12* (4), 981-987.
2. Lowenstam, H.A., Weiner, S. On Biomineralization. Oxford University Press, New York, **1989**.
3. Finnemore A.S., Scherer M. R. J., Langford R., Mahajan S., Ludwigs S., Meldrum F. C., Steiner U. *Adv. Mater.* Nanostructured Calcite Single Crystals with Gyroid Morphologies **2009**, *19* (38-39)**,** 3928-3932.
4. Wucher B., Yue W., Kulak AN, and Meldrum FC, Designer Crystals: Single Crystals with Complex Morphologies. *Chem. Mater.* **2007**, *19* (5), 1111-1119.
5. Yadlovker, D. and Berger, S., Nucleation and growth of single crystals with uniform crystallographic orientation inside alumina nanopores. J. Appl. Phys. **2007,** 101(3), 034304.
6. Beiner, M., G. T. Rengarajan, Pankai, S., Enke, D., Steinhart, M., Manipulating thecrystalline state of pharmaceuticals by nanoconfinement. *Nano Letts.* **2007,** 7(5): 1381-1385.

7. Chen, P. -Y. and Lin, A. Y. M. and Lin, Y. -S. and Seki, Y. and Stokes, A. G. and Peyras, J. and Olevsky, E. A. and Meyers, M. A. and McKittrick, J. Structure and mechanical properties of selected biological materials, *J. Mech. Behav. Biomed. Mater.* **2008**, *1* (3), 208-226.

8. Gunnison, K. E., Mehmet, S., Jun, L. and Ilhan, I. A., Structure-Mechanical Property Relationships in a Biological Ceramic-Polymer Composite: Nacre, *MRS Proceedings.* **1991**, *255*, 171-183.

9. Stephens, C. J., Ladden, S. F., Meldrum, F. C., Christenson, H. K. Amorphous Calcium Carbonate is Stabilized in Confinement. *Adv. Funct. Mater.* **2010,** *20* (13), 2108-21.

10. Bierman, M. J., Lau, Y. K. A., Kvit, A. V., Schmitt, A. L., Jin, S. Dislocation-Driven Nanowire Growth and Eshelby Twist. *Science* **2008,** *320* (5879), 1060-1063.

11. Eshelby, J. D. Screw Dislocations in Thin Rods. *J. Appl. Phys.* **1953,** *24* (2), 176-179.

12. Zhu, J., Peng, H. L., Marshall, A. F., Barnett, D. M., Nix, W. D., Cui, Y. Formation of Chiral Branched Nanowires by the Eshelby Twist. *Nat. Nanotechnol.* **2008,** *3* (8), 477-481.

13. Kim, Y.-Y., Hetherington, N. B. J., Noel, E. H., Kröger, R., Charnock, J. M., Christenson, H. K., Meldrum, F. C. Capillarity Creates Single-Crystal Calcite Nanowires from Amorphous Calcium Carbonate. *Angew. Chem. Int. Ed.* **2011,** *50* (52), 12572-12577.

14. Liu, J., Duan, J. L., Toimil-Molares, M. E., Karim, S., Cornelius, T. W., Dobrev, D., Yao, H. J., Sun, Y. M., Hou, M. D., Mo, D., Wang, Z. G., Neumann, R. Electrochemical Fabrication of Single-Crystalline and Polycrystalline Au Nanowires: The Influence of Deposition Parameters. *Nanotechnology* **2006,** *17* (8), 1922.

15. Dresselhaus, M.S., Lin, Y.-M., Rabin, O., Black, M.R., Kong, J., and Dresselhaus, G., Nanowires. In *Springer Handbook of Nanotechnology*, 3. ed., Bhushan, B., Ed. Springer-Verlag: Berlin Heidelberg, **2010**.

16. Stadelmann, P. *Electron Microscopy Software - Java Version (Jems)*, CIME - EPFL Switzerland, Lausanne, 1999-2011.

17. Chen, Z., Majidi, C., Srolovitz, D. J., Haataja, M. Tunable Helical Ribbons. *Appl. Phys. Lett.* **2011,** *98* (1).

18. Wang, J.-S., Feng, X.-Q., Wang, G.-F., Yu, S.-W. Twisting of Nanowires Induced by Anisotropic Surface Stresses. *Appl. Phys. Lett.* **2008,** *92* (19), 191901-3.

19. Diao, J. K., Gall, K., Dunn, M. L. Atomistic Simulation of the Structure and Elastic Properties of Gold Nanowires. *J. Mech. Phys. Solids* **2004,** *52* (9), 1935-1962.

20. Gall, K., Diao, J. K., Dunn, M. L. The Strength of Gold Nanowires. *Nano Lett.* **2004,** *4* (12), 2431-2436.

21. Qiao, L., Zheng, X. Effect of Surface Stress on the Stiffness of Micro/Nanocantilevers: Nanowire Elastic Modulus Measured by Nano-Scale Tensile and Vibrational Techniques. *J. Appl. Phys.* **2013,** *113* (1), 013508-9.

22. Haiss, W. Surface Stress of Clean and Adsorbate-Covered Solids. *Rep. Prog. Phys.* **2001,** *64* (5), 591.

23. Pokroy, B., Fitch, A.N., Marin, F., Kapon, M. Adir, N., Zolotoyabko, E., Anisotropic lattice distortions in biogenic calcite induced by intra-crystalline organic molecules. J. of Struct. Biol. **2006**, 155(1), 96-103.

24. Cantaert, B., A. Verch, Kim, Y.-Y., Henning, L., Paunov, V., Kröger, R., Meldrum, F.C.M. Formation and Structure of Calcium Carbonate Thin Films and Nano-fibers Precipitated in the Presence of Poly(Allylamine Hydrochloride) (PAH) and Magnesium Ions. Chem. Mater. **2013,** 25(24): 4994–5003.

23. Akatyeva, E., Kou, L. Z., Nikiforov, I., Frauenheim, T., Dumitrica, T. Electrically Active Screw Dislocations in Helical Zno and Si Nanowires and Nanotubes. *ACS Nano* **2012,** *6* (11), 10042-10049.

26. Wang Z. L. Zinc oxide nanostructures: growth, properties and applications. J. Phys. Conden. Matt. **2004**, *16*, R829-R858.